![TU Delft logo]

Delft University of Technology

Quantification and Classification of Short-term Instability Voltage Deviations

Boricic, Aleksandar; Torres, Jose Luis Rueda; Popov, Marjan

Important note
To cite this publication, please use the final published version (if applicable).
Please check the document version above.

Quantification and Classification of Short-Term Instability Voltage Deviations

Aleksandar Boričić ⬤, *Member, IEEE*, Jose Luis Rueda Torres ⬤, *Senior Member, IEEE*, and Marjan Popov ⬤, *Fellow, IEEE*

Abstract—As power systems evolve from synchronous to inverter-based generation, short-term voltage stability evaluation plays an increasingly important role. Voltage perturbations become faster and highly variable, exposing systems to much larger risks of cascading faults. Therefore, assessing the severity and origin of potential voltage deviations becomes a critical step in risk-based vulnerability analysis of modern power systems. In this article, a novel approach that evaluates rapid post-fault voltage deviations for both online and offline short-term instability quantification and classification is investigated. The findings indicate that the approach is intuitive and effective in automatically determining the severity and type of instability. Such an output enables grid operators to anticipate and prioritize potential high-risk events and act with suitable preventive and/or corrective actions. Finally, the article provides future research directions that deal with the open grid resilience challenges. Particularly, the challenges related to post-disturbance dynamic system strength evaluation are addressed.

Index Terms—Classification, inverter-based resources, power system stability, quantification, short-term voltage stability, synchrophasors, system strength.

I. INTRODUCTION

WORLDWIDE, electric power systems experience rapid and unprecedented changes that often lead to the operation closer to system stability limits. The increased system complexity is seen on both the production and the demand side. On the production side, the proliferation of Inverter-Based Resources (IBR) and Distributed Energy Resources (DER) introduces a very different post-fault system response, potentially jeopardizing its resilience and contributing to vulnerability [1], [2], [3]. On the demand side, the accelerating electrification and the application of power electronics components lead to a more complex response that cannot be modelled simplistically [3], [4]. This affects both system stability and grid operation [5].

Whilst the stability of the conventional power systems was fundamentally related to the frequency and rotor angle stability of synchronous machines, the stability of the IBRs, the penetration of which continuously increases, is primarily judged by voltage performance. When voltage experiences perturbations, it is more likely for the IBRs to disconnect, desynchronize, or fail to support the grid. As this tends to occur in already-severe voltage conditions, it may further exacerbate the situation. Additionally, the reduction of synchronous generation simultaneously leads to lower system strength. This makes the evaluation and the quantification of voltage deviations and stability a very important subject [6], [7].

Therefore, modern power systems become much more voltage-sensitive, and for a system with a high penetration of power electronics that mostly relies on stiff voltages, short-term voltage stability is of paramount importance. This article discusses how these structural system changes should also change the way we evaluate and quantify short-term stability.

To evaluate short-term instability, the current practice is to typically focus on the binary representation of (in)stability. Grid operators define relatively straightforward voltage-time thresholds, and when a voltage deviates outside of these thresholds, it is deemed unstable. For instance, in the US, the Western Electricity Coordinating Council (WECC) defines fixed thresholds depending on the type of event [8]. In the EU, Transmission System Operators (TSOs) define instability thresholds differently, sometimes based on ride-through criteria in the grid codes [9]. Such approaches are not intended nor applicable to quantify the severity of voltage deviations.

Other advanced short-term instability methods typically focus on monitoring instability-specific metrics such as rotor angles [10], load admittances [11], or frequency and damping of oscillations [12]. Alternatively, [13] evaluates the transient IBR stability using Lyapunov's method, while [14] reviews several stability methods and challenges in IBR-rich grids.

In this article, the problem is analyzed from a very different and novel perspective, by utilizing the information available in post-fault voltage deviations of short-term instability events. The main contributions of the article are summarized as follows:

- Various mechanisms of short-term instabilities and their evolution and importance in modern IBR-rich power systems are discussed, described, and concisely categorized.
- A novel and widely-applicable method for quantifying the severity of short-term voltage deviations is introduced.
- The method is tested extensively on a comprehensive set of dynamic simulations and is compared against a common existing method, exhibiting superior performance.
- To complement the introduced quantification algorithm, a classification algorithm is developed which performs with high accuracy by relying on voltage trajectories only.
- The combined algorithms are able to quantify and evaluate the severity level of short-term instabilities and provide information on the type of event. Such insights can be used for automated risk-based vulnerability assessment, which is discussed in the final section as a topic of future work.

The article is organized as follows. Section II provides background on relevant short-term instability mechanisms and their interaction with the increased penetration of the IBR penetration. Section III introduces a novel method for the real-time evaluation and quantification of instabilities presented in Section II. In Section IV, the test setup is elaborated, followed by a comprehensive analysis and discussion. Furthermore, in Section V, a novel classification algorithm is introduced to complement the quantification method. Finally, Section VI concludes the article and discusses future research possibilities that are enabled by the newly introduced method.

II. SHORT-TERM INSTABILITY IN MODERN POWER SYSTEMS

For conventional power systems, short-term instability was mainly understood as either Short-Term Voltage Instability (STVI) or Transient Rotor Angle Instability (TRAI) [15]. The former is commonly a consequence of post-fault loss of equilibrium in load-system interactions, particularly dynamic loads. A possible disturbance causes motor deceleration, and in certain cases, instability may occur, characterized by a rapid voltage collapse. Prior to the potential collapse, oscillations may also occur because of interactions between the dynamic load restoration and synchronous generators' (SG) voltage regulators. Therefore, to analyze STVI appropriately, a detailed representation of dynamic loads is needed. The onset of STVI typically occurs after a fault in areas with a high share of the (dynamic) load. The instability can be also related to HVDC dynamics, and more recently, IBR and/or DER dynamics [2].

TRAI, on the other hand, is an SG-related event. A disturbance, typically short-circuit in tie lines and/or near SGs, could cause the rotor angles of the generators (or generator groups) to drift sufficiently far from each other to lose synchronism. The instability can be either a first swing instability or instability occurring after a few cycles of oscillations. The latter is more common for larger systems with many SGs. The usual frequency of these electromechanical oscillations is up to 2.5 Hz [2].

These two forms of instability, STVI and TRAI, are still present in modern systems, but they become intertwined with new IBRs' and load dynamics. Therefore, to describe the short-term stability of modern systems, new subtypes of short-term instability are emerging [2].

One of them is Fault-Induced Delayed Voltage Recovery (FIDVR). FIDVR is characterized as a post-fault depressed voltage, lasting typically from several seconds up to tens of seconds, jeopardizing the overall system's ability to recover. This is mainly attributed to the stalling of large amounts of induction motors, particularly the A/C units [16]. After the stalled motors get disconnected by the overcurrent or thermal protection, an overvoltage situation may arise. FIDVR is not an instability on its own, as the system may succeed in recovering in some cases, but the voltage consequences of FIDVR present a major threat to cascading. Conceptually, FIDVR can also be described as a less severe specific type of STVI, as it is fundamentally related to motor stalling. Furthermore, FIDVR can be affected and possibly exacerbated by DER operation, particularly inverter blocking or disconnection [3], [17].

Another newly introduced form of short-term instability is converter-driven instability. It can manifest itself in terms of fast interactions (hundreds of Hz), and slow interactions (typically around 10 Hz or less) [2]. The latter, Converter-driven Slow-Interactions Instability (CSII), is further considered in this article, while the former is out of scope. CSII usually emerges in "weak" system sections, where voltage is very sensitive to changes in active and reactive current/power. After a disturbance, the inverter controls may not be able to "lock" onto grid voltages correctly, resulting in voltage oscillations. Additionally, as more inverters are introduced in the systems, there is more chance of undesired interactions, sometimes leading to oscillatory behavior and possible voltage collapse if undamped. The post-fault converter-related instabilities have been an increasingly relevant subject worldwide, particularly (but not exclusively) in the systems with already high (local) IBR penetration and with consequent system strength reduction, such as in Australia, Texas, California, China, or the United Kingdom [18].

The four described phenomena (STVI, TRAI, FIDVR, and CSII) are concisely described in Fig. 1. All four phenomena are distinctive in the location where they typically emerge, the origin of instability, the way of manifesting itself, and ultimately the actions that can be taken to prevent them. However, they also have many common characteristics:

- Manifestation in a similar time scale (usually < 10 s),
- All of them lead to significantly disturbed (but distinctive) post-fault voltage deviations,
- They often interact with each other when a potential system instability takes place,
- They become more common and more severe due to the introduction of more inverter-based resources and reduction of system strength,
- May lead to cascading events and system blackouts.

As the instability phenomena become more entangled, the risks of cascading increase accordingly [2], [3]. However, the present evaluation techniques typically focus on analyzing, quantifying, and predicting instabilities individually. This may not be optimal considering intertwined voltage dynamics seen
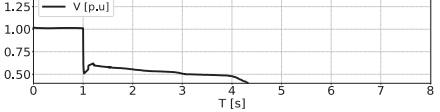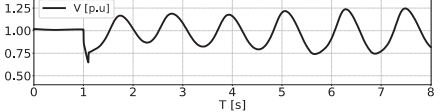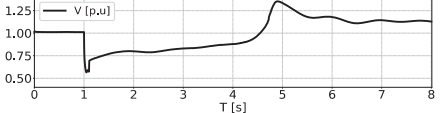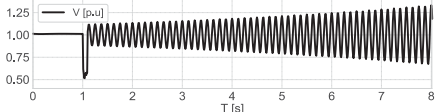
Instability Mechanism	Distinctive Characteristics of Each Short-Term Instability Phenomenon		
	Typical Location	Typical Dynamical Causes and Effects	Typical Post-Fault Voltage Deviation
Short-Term Voltage Instability (STVI)	Grid sections with high amounts of (dynamic) load and DER;	Motors dynamics and stalling; HVDC links dynamics; IBR and DER dynamics; Combination of any of the above;	
Transient Rotor Angle Instability (TRAI)	Tie-lines; Near-SG buses;	Large rotor angle deviations; Low CCT - loss of synchronism; Electromechanical oscillations (<2.5Hz);	
Fault-Induced Delayed Voltage Recovery (FIDVR)	Areas with a high share of dynamic load (particularly A/C units) and DER;	Massive induction motors stalling (mostly A/C) and disconnection; Massive DER disconnection and/or blocking;	
Converter-driven Slow Interactions Instability (CSII)	Remote or "weak" grid sections (low strength); Areas with many IBRs; High IBR control gains;	Interactions between IBR/DER controls, grid, and SG controls; Interactions with dynamic load; Oscillations (typically 7-10Hz range);	

Fig. 1. Concise overview of the four short-term instability phenomena, characteristics, and illustrative post-fault voltage deviations.

more commonly in modern power systems, which will be exemplified in Section IV. The quantification of various types of short-term instabilities is not only preferred but also necessary to preserve the stability of renewables-driven power grids in various operational scenarios. Before any smart preventive and corrective strategies can be introduced, the effects should be quantified and accurately predicted.

In this article, the severity of short-term instabilities is evaluated with a novel voltage-based quantification method: the cumulative voltage deviation (CVD) metric. Such an approach is applicable and relevant for all short-term instability mechanisms, even in grids with a high share of IBRs and dynamic loads. The method is introduced in Section III and tested extensively with dynamic simulations in Section IV.

III. QUANTIFICATION METHODOLOGY

The research on short-term instabilities has been a topic of interest for many years, although the field is still immature in comparison to long-term stability evaluation [19]. As electrical power systems experience lower inertia and lower system strength, system dynamics are inevitably enhanced. Furthermore, as described in Section II, IBR-dominated grids are voltage-sensitive. Therefore, evaluating and quantifying short-term voltage deviations becomes much more relevant.

Concurrently, the accelerating application of Phasor Measurement Units (PMUs) drastically changes the real-time monitoring and control landscape [20]. What used to be impossible due to the slow SCADA sampling (typically one unsynchronized measurement per 1-3 seconds), is now much more feasible with time-synchronized and fast wide-area measurements (typically 50 or more measurements per second). This opens a completely new range of possibilities for monitoring and vulnerability assessment analysis in modern power systems.

Nonetheless, some existing methods deal with short-term instability evaluation. We omit a detailed overview for brevity and refer readers to [19] and [21], where the most common methods have been analyzed, including their shortcomings when applied to modern power systems. Some of the conclusions were that a new quantitative metric is necessary for IBR-rich systems, which should meet the following conditions:

- Able to detect and quantify the severity of various post-fault short-term voltage deviations,
- Useful in both conventional and converter-dominated power systems,
- Intuitive for practical on- and off-line applications,
- Adaptable to any system and operational scenario,
- As simple and computationally efficient as possible,
- Can provide real-time insights into post-fault stability, for instance by relying on PMU data.

To address these challenges, this article introduces the Cumulative Voltage Deviation (CVD) method, visualized in Fig. 2 and mathematically described by (1)–(3).

$$V_U(t) = (1 + a) V_0 - t/b \tag{1}$$

$$V_D(t) = (1 - a) V_0 + t/b \tag{2}$$

$$CVD = \sum_{t=t_f}^{t=t_f+T} \begin{cases} V(t) - V_U(t), & if \ V(t) > V_U(t) \\ V_D(t) - V(t), & if \ V(t) < V_D(t) \\ 0 & , \ else \end{cases} \tag{3}$$

In (3), t_f is the fault inception time, and T is the evaluation time window. $V_U(t)$ is the up threshold (blue dashed line in the upper graph in Fig. 2), whereas $V_D(t)$ is the down threshold (the orange dashed line of the lower graph in Fig. 2).

The CVD evaluation starts once the voltage overshoots the initial threshold (shown as points A or C in Fig. 2), indicating a disturbance that may potentially lead to instability. The linear
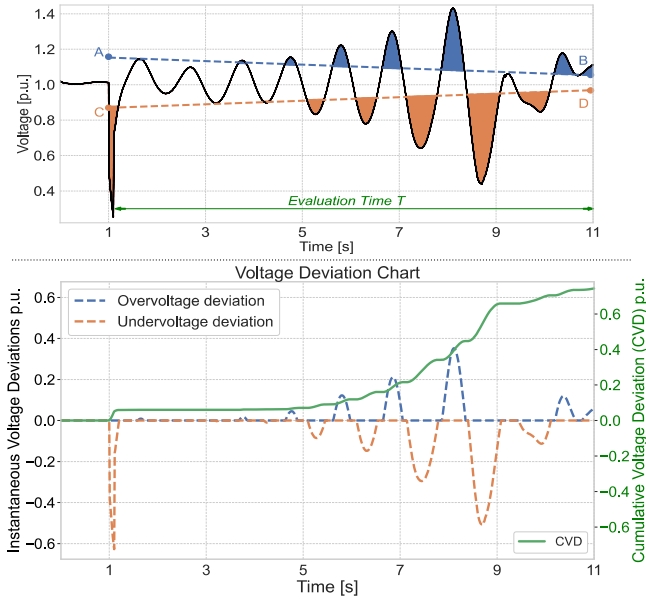
Fig. 2. Visualization of the CVD method for an illustrative case of voltage oscillations related to post-fault TRAI.

envelope threshold is then applied to quantify the severity and duration of the detected voltage deviations. Based on this threshold, the post-disturbance voltage deviations are disentangled into undervoltages (orange areas in Fig. 2) and overvoltages (blue areas in Fig. 2), and extracted onto a voltage deviation chart (the lower plot of Fig. 2). The green line of the lower plot represents CVD, i.e., the cumulative sum of over- (blue) and under-voltage (orange) deviations. Therefore, the final CVD value reflects the total amplitude and time of the voltage deviations outside the predefined limits.

The linear threshold is chosen as it exploits the fact that voltage deviations in the late (early) post-disturbance phase are more (less) indicative of instabilities. In other words, initial large post-fault voltage transients are to be expected, however, when the voltage deviations do not decrease sufficiently fast during the post-fault period, it indicates a larger probability of instability. Furthermore, the method is straightforward, computationally fast, and valid for any system or short-term instability scenario addressed in Fig. 1, which will be shown in Section IV. Finally, as it relies solely on voltage measurements, it is applicable not just to offline, but also to online studies, by utilizing PMU measurements.

A short-term instability monitoring method should be easy to parametrize and apply to various systems [21]. The CVD method requires setting only three simple parameters. The first is the evaluation time denoted with T. As described in Section II, the majority of the phenomena in question occur within ten seconds, therefore chosen as a T value. Such a value is also commonly used for short-term studies [2]. The other two parameters are a and b. They define the initial points (A and C in Fig. 2), and the final points (B and D in Fig. 2), including the slopes of $V_U(t)$ and $V_D(t)$. To detect and quantify severe voltage deviations of the four types introduced in Section II, we propose

$a = 0.15$ and $b = 100$. Practically, this means that the evaluation starts when the voltage overshoots $\pm$ 15% from the pre-fault voltage ($t \approx t_f$) moving towards $\pm$ 5% ($t = t_f + T$), with a slope of 1%/s. Such values are chosen as they represent common thresholds for large voltage disturbances and recovery values, respectively, and at the same time efficiently capture various short-term phenomena, as highlighted in Section IV. Finally, V_0 is the pre-fault voltage, calculated as an average value prior to the fault. To ensure that the pre-fault voltage value is not impacted by the fault transients or initial model transients, a half-a-second pre-fault window [0.4–0.9 s] is used.

The effectiveness and the applicability of CVD to detect and quantify the severity of various short-term voltage deviations with the selected parameters are analyzed in Section IV.

IV. RESULTS AND DISCUSSION

In this section, the efficacy of the CVD is evaluated on a large number of dynamic simulations utilizing DIgSILENT PowerFactory supported by Python scripting [22]. The CVD method is assessed for various instability phenomena described in Section II and compared to an existing commonly used metric for quantification of voltage deviations [21].

To obtain a relevant analysis and comparison, a large number of dynamic post-fault voltage trajectories is needed. For this task, IEEE Test System for Voltage Stability Analysis and Security Assessment is used [23]. This test grid is currently one of the most advanced large test grids for dynamic voltage stability simulations and is extensively used in research on related topics. The system is further enhanced by introducing a large number of WECC Composite Load models, necessary to improve the accuracy of grid and load dynamics [3], [24]. The model is depicted in Fig. 3.

All the simulations are performed for 100 ms three-phase faults at bus 4044 with a fault impedance of 2.5 Ω unless stated differently. A large number of scenarios are selected based on the analysis conducted in [3], which demonstrated the system conditions and parameters that lead to relevant instabilities in this grid. The voltage responses are reported for bus 1041, with comparable results to other buses susceptible to voltage instability in the central area [3], [23].

The CVD method, as per parameters from Section III, is compared to the Transient Voltage Severity Index (TVSI), which is commonly used in the literature for quantifying post-fault transient voltage deviations [25]. The TVSI method for a specific bus is mathematically straightforward and is described in (4) and (5), where T is the analyzed transient time frame, T_C is the fault clearing time, TVDI is the Transient Voltage Deviation Index, $V_{i,t}$ is the voltage magnitude of the bus i at time t, and μ is the threshold used to define the unacceptable voltage deviation level.

$$TVSI = \frac{\sum_{t=T_c}^{T} TVDI_{i,t}}{(T - T_c)} \quad (4)$$

$$TVDI = \begin{cases} \frac{|V_{i,t} - V_{i,0}|}{V_{i,0}}, & if \quad \frac{|V_{i,t} - V_{i,0}|}{V_{i,0}} \geq \mu \\ 0, & otherwise \end{cases} \quad \forall t \in [T_c, T]$$
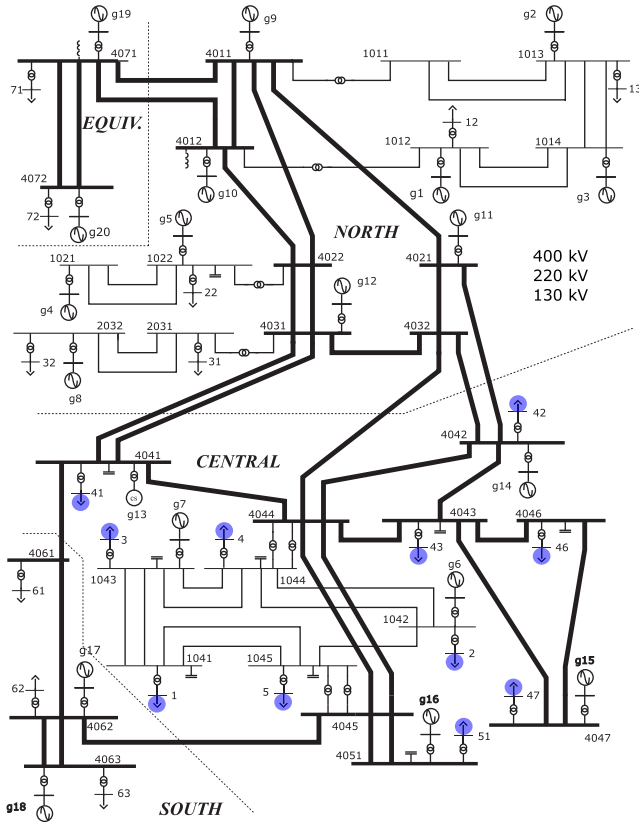
$$(5)$$

Fig. 3.   IEEE test system for voltage stability analysis and security assessment, with blue circles indicating WECC composite load additions. See [23] and [3] for details about the grid and test cases.

TABLE I
PARAMETERS USED TO MODEL FIDVR EVENTS

Simulation number	Dynamic load penetration [%]	Share of motor type D [%]
0	16%	36%
1	17%	37%
2	18%	38%
…	…	…
24	40%	60%

According to [25], a threshold of $\mu = 20\%$ is adopted for analysis and comparison purposes. Further information about this method can be found in [21], [25].

A. Fault-Induced Delayed Voltage Recovery (FIDVR)

The analysis commences with FIDVR simulations. Our experience shows that the best way to simulate FIDVR events is to introduce a large number of stalling-prone dynamic loads, particularly single-phase A/C units; the more loads, the more severe the FIDVR event is [3]. By taking this into account, a range of 25 dynamic simulations is conducted with increasing severity, by controlling two parameters: (i) the overall dynamic load percentage in the grid; and (ii) the percentage of motor type D (single-phase A/C units) in the WECC composite loads. The varying FIDVR simulation parameters are listed in Table I. The

TABLE II
PARAMETERS USED FOR MODELING TRAI EVENTS

Simulation number	Dynamic load penetration [%]	Fault clearing time (100ms default) [ms]
0	36%	200
1	37%	200
2	38%	200
…	…	…
24	60%	200

share of A/B/C-type motors in the dynamic loads is set to 0.1 for all simulations to replicate realistically diverse system loads, based on the methodology reported in [3].

The results are shown in Fig. 4(a) and (b). The plots in Fig. 4(a) show the increasingly severe FIDVR voltage events, starting from the least severe (shown in dashed red). The corresponding CVD and TVSI thresholds are depicted in the plots with dashed lines.

Fig. 4(b) depicts a scatterplot that quantifies the total severity of the events (normalized to event 0), for CVD and TVSI. The events are reported on the X-axis from the least severe (leftmost, simulation number 0), to the most severe (rightmost, simulation number 24), as per Table I.

It can be seen that TVSI reaches a peak at event number 12, inaccurately indicating that the events that follow are *less* (not more) severe. Meanwhile, CVD successfully quantifies the increasing severity, presenting a linear rise. This can be explained by a few key differences between the two approaches: (i) TVSI is, unlike CVD, unable to take into account the time-increasing voltage characteristics of FIDVR; (ii) the overvoltage deviations in the late FIDVR phase, which can be detrimental to the system's ability to recover, are much better evaluated by CVD; and (iii) CVD threshold depends on the pre-fault voltage, unlike TVSI, which helps in adapting the linear thresholds more accurately to the specific event.

Overall, it can be concluded that FIDVR events of increasing severities are adequately quantified by the CVD approach, which shows much better performance than TVSI.

B. Transient Rotor Angle Instability (TRAI)

To simulate TRAI events, the system needs to be stressed electromechanically so that synchronous machine(s) begin to oscillate against each other. For the system shown in Fig. 3, this can be achieved by applying a fault at bus 4062, which results in oscillations of generators g17 and g18 against the rest of the system. To model increasingly severe post-fault oscillations, parameters shown in Table II are utilized, where dynamic load penetration is continuously increased. The share of A/B/C-type motors in the WECC dynamic load model is set to 0.3/0.2/0.3 in this set of simulations to emphasize their impact on post-fault voltage deviations, as per analysis performed in [3]. The results are illustrated in Fig. 4(c) and (d).

In Fig. 4(c), post-disturbance TRAI events are plotted, with increasing severity as more dynamic loads are introduced. The system eventually reaches a stable equilibrium, however with a
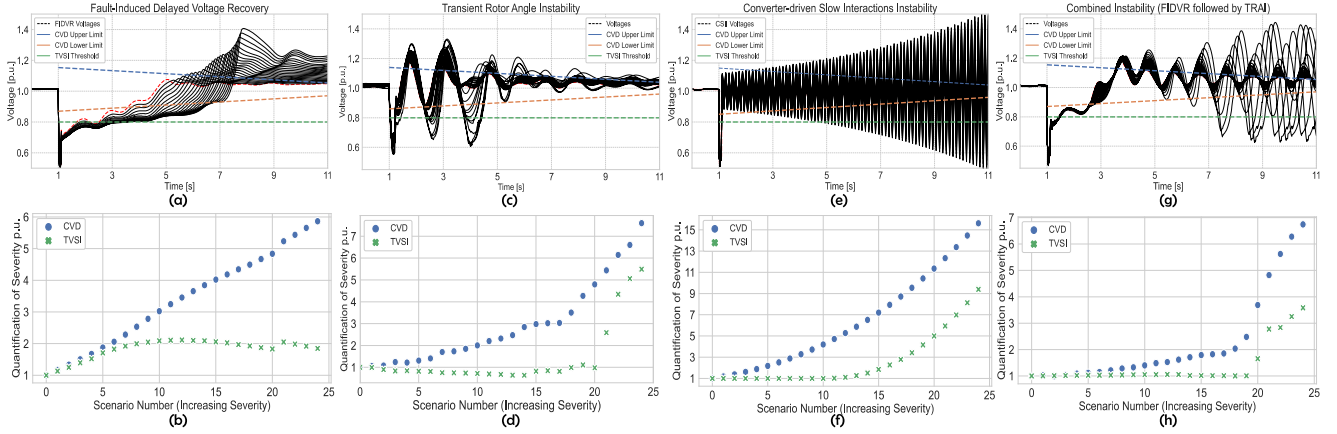
Fig. 4. Comparison of CVD and TVSI; upper plots show dynamic simulations (black) with increasing severity (starting from red dashed line). The scatterplots show corresponding quantification (normalized) of CVD voltage deviations (blue circles) and TVSI (green crosses).

rising severity of voltage deviations, indicating a higher risk of cascading and collapse. For completeness, another case with an unstable long-term equilibrium is studied in Section IV-D. The rising severity of responses in Fig. 4(c) is reflected by CVD and TVSI values, with a visualized comparison in Fig. 4(d).

By observing the trends in Fig. 4(d), it can be seen that TVSI has a downward trend up until simulation number 15, wrongly indicating that events are getting less (not more) severe. This is despite oscillations becoming more pronounced with a potentially higher impact on system stability. Only after simulation number 20 is the increased severity correctly picked up by TVSI. Meanwhile, CVD correctly evaluates that the system is experiencing more severe voltage deviations throughout all simulations, with no issues in describing the rising severity trend in simulations. Hence, CVD performance is significantly better for TRAI events. The improvement is achieved since CVD, unlike TVSI, evaluates both over- and undervoltages, while it also applies a time-adaptive linear threshold which tracks and quantifies the voltage response more accurately, as seen in Fig. 3(c) and discussed in Section III.

C. Converter-driven Slow Interactions Instability (CSII)

To model severe CSII events, electromagnetic transient (EMT) simulations would be necessary, as any RMS-modelled events above ∼5 Hz are unlikely to be accurately captured [26]. Furthermore, realistic CSII voltage deviations are generally difficult to model, as they are often a consequence of complex control interactions in weak grids. As RMS simulations on the system from Fig. 3 are performed in this article, a different approach to derive suitable voltage profiles is used. Relying on the current understanding of CSII phenomena [2], and according to the recent CSII events from Texas, Australia, and Scotland [18], synthetic events are created analytically, with post-clearing voltage defined by (6).

$$V(t) = Ae^{\beta t}\cos(2\pi ft) + 1 \quad ; \quad for\ t > t_{cl} \qquad (6)$$

The two parameters, initial amplitude A and exponential coefficient β, are defined in a range of values, as shown in

TABLE III
PARAMETERS USED TO MODEL CSII EVENTS

Simulation number	Amplitude A	Exponential coefficient β
0	0.052	0.05
1	0.054	0.054
2	0.056	0.058
…	…	…
24	0.100	0.150

Table III. The values are chosen to replicate potential CSII events as accurately as possible, based on real grid events [17], while at the same time providing increasing severity in terms of amplitude and exponential rise in the post-fault period.

The derived voltages are shown in Fig. 4(e) and (f). The synthetic voltage profiles match very well with the ones seen in EMT analyses or field measurements [6], [18]. The least severe voltage profile is plotted in dashed red for clearer visualization, whereas every following event has a higher amplitude and exponential rise, as shown in Table III.

In Fig. 4(f), the quantification of these events is shown for CVD and TVSI. Starting with TVSI, one can see that the increasing severity is accurately quantified only from event number 13. Before this event, the sensitivity of TVSI is insufficient to differentiate among the events of various severities, resulting in an inaccurately flat severity trend. On the other hand, CVD is sensitive enough to pick up the differences even amongst the first few events and continues to quantify increasing severity for all the events. These improvements seen in CVD relative to TVSI are a consequence of analogous reasons as with FIDVR and TRAI.

Furthermore, the ability to put more weight on voltage deviations further away from the fault clearing benefits CVD over TVSI, which becomes very important in exponentially growing oscillatory behaviour.

The frequency of the oscillations f is chosen to be 8 Hz, as the frequency range of CSII is typically 7–10 Hz [6], [18]. The results are not sensitive to this assumption and hold equally for

TABLE IV
PARAMETERS FOR COMBINED INSTABILITY EVENTS

Simulation number	Dynamic load penetration [%]	Fault clearing time (100ms default) [ms]
0	38%	125
1	38.5%	125
2	39%	125
…	…	…
24	50%	125

other CSII event frequencies. This is analysed but unreported in the article for brevity. From the overall results, it can be seen that CVD is very suitable for quantifying the severity of CSII-related post-fault voltage deviations.

D. Combined Instability (FIDVR + TRAI)

For the final round of presented simulations, a case of intertwined instabilities is considered. As discussed in Section II, the structural changes of the power systems lead to more interactions among different instability phenomena, resulting in a risk of cascading instabilities, which is illustrated here.

The simulations in this subsection are, once again, performed on the IEEE test system from Fig. 3. To produce cases of entangled instabilities, two changes are introduced in the model: (i) a high and increasing amount of dynamic load is added, and (ii) an increased fault clearing time. Table IV shows the events taken into consideration.

The share of A/B/C/D-type motors in the dynamic loads is set to 0.1/0.1/0.3/0.1, respectively, for all simulations, which is in line with the methodology reported in [3]. The values are chosen in a way to produce the combined instability scenarios.

The results are shown in Fig. 4(g) and (h). All the events show an initial short-lasting FIDVR event (up to ~3-4 seconds), followed by electromechanical oscillations which indicate a risk of TRAI. The simulations are sorted in an increasing severity order, as shown in Table IV. This can be seen in the progressively more severe FIDVR and stronger voltage oscillations, starting from the least severe case (dashed red). Such complex grid instability phenomena are more likely to emerge in modern grids, as discussed in Section II, for instance, in low inertia grids with a high share of dynamic load.

From the Fig. 4(h) scatterplot, one can again note that CVD performs much better than TSVI in quantifying the severity of these voltage deviations. TVSI shows almost no sensitivity to the increasing severity up to event number 20, which is already a very severe one. It even shows a slight downward trend, wrongly indicating a reduction in severity. The last five events are the most severe as TRAI rapidly unfolds, followed by low-frequency but extremely high-amplitude voltage deviations that are followed by out-of-step conditions and potential system instability. CVD can again correctly distinguish between various events of different severity by utilizing the proposed time-adaptive linear voltage thresholds.

The results from the four analysed instability mechanisms show unanimously how a cumulative voltage deviation is an efficient approach to quantify post-voltage deviations. The method performs notably better than the commonly used severity index TVSI, with much less risk of underestimating an event, irrespective of the instability type.

V. CLASSIFICATION OF VOLTAGE DEVIATION EVENTS

In Section IV, the quantification of various disturbances based on the voltage deviation severity is introduced [27]. However, such an approach addresses only the voltage event severity, without providing more insight into the type of event taking place. This section explores the latter further.

The theoretical classification and characterization of disturbances and instabilities is an important topic in academia and industry [2]. However, approaches that focus on short-term instabilities are rarely investigated [19], and are emerging as major challenges for the resilient operation of IBR-dominated power systems [1], [2], [3], [4], [5], [6], [7]. Some existing data-based classification approaches rely on statistics, clustering, regressions, and other machine learning (ML) techniques to detect and classify disturbances [28], [29], [30], [31] rapidly. Moreover, oscillation detection algorithms have been proposed based on approaches such as the Prony method, the Hankel Total Least Square method, the Matrix Pencil method, and the Wavelet transform [32], [33], [34], [35]. Non-oscillatory instability events such as FIDVR are typically detected based on voltage or admittance monitoring [36], [37]. STVI detection is discussed extensively in [21].

Most of the short-term instability classification methods, therefore, focus on detecting a specific type of disturbance or instability, rather than on classifying various disturbances in simulation results or in real-time.

This section introduces a novel classification algorithm for short-term instabilities that complements the CVD quantification method presented in Sections III and IV. Similarly to the CVD quantification algorithm, the classification algorithm is designed to be robust and perform based on voltage inputs only. This makes it applicable not only for rapid scripted stability studies by applying tools such as DIgSILENT PowerFactory and Python [22], but also for real-time applications with synchrophasors [31]. The algorithm is designed to distinguish between the four types of short-term instabilities described in Fig. 1 with high accuracy.

The high-level overview of the entire quantification and classification algorithm process is shown in Fig. 5. The first three steps are already explained in the previous sections. The implementation of steps 4 and 5 is hereby discussed in detail.

A. Classification Methodology and Implementation

As described in Section I and Fig. 1, there are four distinctive short-term voltage instabilities: Short-Term Voltage Instability (STVI), Transient Rotor Angle Instability (TRAI), Fault-Induced Delayed Voltage Recovery (FIDVR), and Converter-driven Slow Interactions Instability (CSII). All these phenomena
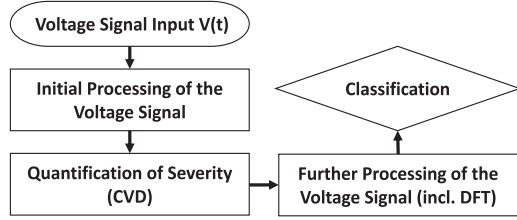
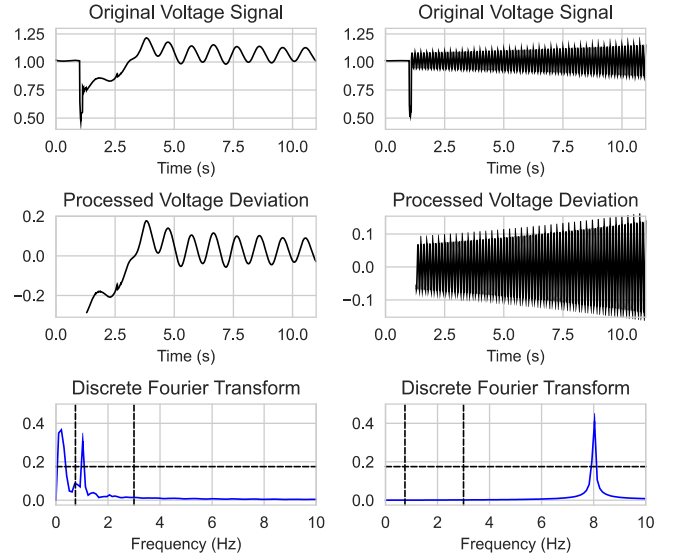Fig. 5. Overview of the quantification and classification algorithms.

Fig. 6. Example of implementing the DFT-based classification. Scenario combined instability no. 15 (left), and scenario CSII instability no. 5 (right); see Section IV for more details. Dashed lines depict PFM thresholds (horizontal) and frequency bands (vertical).

have unique characteristics that can be exploited to differentiate between them in the classification algorithm. The four types are initially split into two groups: oscillatory and non-oscillatory phenomena. TRAI and CSII fall into the former category, while STVI and FIDVR fall into the latter. These two categories are discussed further.

For the classification of the two oscillatory phenomena (TRAI and CSII), the suggested algorithm pre-processes and transforms the time-series signal into the frequency domain. This is achieved by using Discrete Fourier Transform (DFT), based on the well-known algorithm from [38], hereby implemented in Python using the NumPy library. The pre-processing involves three steps: i) extracting the post-fault voltage deviation signal; ii) removing the first 300 ms to avoid the initial fault transients' impact on DFT accuracy; and iii) removing the DC offset by deducting the mean from the signal. The last step is also implemented to improve the DFT accuracy, as the DC offset is not of interest for classification.

After the frequency domain signal is derived, the algorithm calculates two variables used for classification: Peak Frequency Magnitude (PFM) and Energy Spectral Density (ESD), shown in (7)–(10) for TRAI and CSII, respectively. PFM is the magnitude of the oscillations in the relevant frequency band, while ESD is based on Parseval's theorem of unitary Fourier transform, representing the energy of a signal over a frequency band. $X[k]$ is the signal in the frequency domain, calculated as the DFT of $V(t)$.

$$PFM_{TRAI} = \max\left(X[k]\right); \quad k \in [0.75, 3] \text{ Hz} \quad (7)$$

$$PFM_{CSII} = \max\left(X[k]\right); \quad k > 3 \text{ Hz} \quad (8)$$

$$ESD_{TRAI} = \sum_{k=0.75}^{3} |X[k]|^2 \quad (9)$$

$$ESD_{CSII} = \sum_{k=3}^{max(k)} |X[k]|^2 \quad (10)$$

These two variables are calculated inside two frequency bands: 0.75 Hz to 3 Hz, and > 3 Hz. The choice of such bands is directly related to the inherent differences between TRAI and CSII phenomena. As described in Fig. 1, TRAI voltage deviations are *electromechanical* by nature, and therefore much slower, typically appearing in the mentioned frequency interval [2]. These oscillatory dynamics in power systems are known as

modes [39], and are mathematically described in (11):

$$y_i(t) = A_i^{\sigma_i t} \sin\left(\omega_i t + \phi_i\right) \quad (11)$$

where ω_i is the imaginary part of the complex eigenvalues λ_i, related to the oscillation frequency f_i as shown in (12):

$$\lambda_1 = \sigma_i + j\omega_i \quad ; \quad f_i = \omega_i/2\pi \quad (12)$$

There are three types of electromechanical oscillation modes related to rotor angle instability: i) local-area, ii) intra-station, and iii) inter-area modes [40]. These modes have natural frequencies f_i below 3 Hz due to inherent structural characteristics of power systems and synchronous machines [41]. This can be evaluated with a modal (eigenvalues) analysis.

Meanwhile, CSII is generally a sub-synchronous oscillation phenomenon, and by nature, is almost exclusively *electromagnetic*. As such, it often appears in the 7-10 Hz frequency range [6], however, it can also take other (typically larger) values in the sub-synchronous range [2], [18]. These oscillations are often a consequence of control interactions or PLL performance, particularly in weak grids [26], [42], and are fundamentally distinct from TRAI oscillations [2]. This reflects in their higher frequency, hereby utilized for classification.

For this analysis, the threshold used for both PFM and ESD is set to 0.175 per unit, based on extensive simulation results of the analysed system in Fig. 3. The frequency bands and thresholds can be fine-tuned for the system in question for better performance–for instance by knowing the size of the system and expected electromechanical oscillation modes [2]. If the dominant modes of interest in the analysed (large) system are low-frequency inter-area modes, the lower frequency threshold can be reduced for improved classification accuracy. The entire classification process is exemplified in Fig. 6 for scenarios number 15 from combined instability (left) and scenario number 5 from the CSII events (right), both from Section IV. These

scenarios are taken as illustrative examples; similar analyses and conclusions hold for other scenarios. In Fig. 6, for both left and right-side graphs, black plots are in the time domain, while blue plots are in the frequency domain.

In Fig. 6 right side plots, it can be seen how the voltage signal (upper plot) is firstly processed (middle plot) and then transformed to the frequency domain (lower plot). The DFT graph (blue) shows that the PFM of the oscillations is at 8 Hz with amplitude above the threshold. Furthermore, the ESD value calculated based on (10) is also above the threshold (not shown in graphs), which results in a unanimous decision to classify this event as CSII. On the left side of Fig. 6, a combined instability plot is depicted, which contains a TRAI event. From the DFT, it can be seen that the PFM and ESD are both concentrated inside the 0.75–3 Hz frequency band, with PFM crossing the threshold at around 1 Hz. There is also a peak in the disregarded < 0.75 Hz range but is not of interest as it originates from the initial FIDVR recovery of the combined instability scenario. In this case, the ESD value is below the threshold, however, as the algorithm only needs one value over the threshold (PFM or ESD), it is also correctly classified as a TRAI event. This is a good example to show the benefit of using both PFM and ESD since a signal in the frequency domain could have high PFM but low ESD (high kurtosis), or low PFM but still high ESD (low kurtosis). The latter may occur when the frequency of oscillations is slightly changing throughout the event, or if the data acquisition is less precise or with a lower sampling frequency. By utilizing both values in the classification algorithm, the accuracy of detecting oscillatory events such as TRAI and CSII can be increased notably.

For non-oscillatory events (FIDVR and STVI), a different approach is used, as DFT would not provide a useful differentiator due to the non-oscillatory nature of the events. Instead, these events can be detected and classified in the time domain, by taking advantage of the CVD algorithm introduced in Section III. Firstly, the algorithm is used to determine whether a prolonged undervoltage condition takes place. This is achieved by using the two following conditions: i) if undervoltage CVD (CVD_{UV}) is larger than 75% of the total CVD value, and ii) if CVD_{UV} is larger than 0.03 per unit. Both conditions are applied only to the first 3 seconds of the post-fault signal and are described in (13) and (14).

$$\sum_{t=t_f}^{t_f+3} CVD_{UV}(t) > 75\% * CVD \tag{13}$$

$$\sum_{t=t_f}^{t_f+3} CVD_{UV}(t) > 0.03 \, p.u. \tag{14}$$

The reasoning behind the two utilized conditions has both theoretical and experimental foundations. The first condition, shown in (13), is used to differentiate between oscillatory and non-oscillatory events. In the first few seconds of STVI and FIDVR, the undervoltage deviation is the dominant type relative to the overvoltage deviation (see Section I and Fig. 1). When a significant overvoltage also exists, the event is likely of an oscillatory nature instead (TRAI or CSII). Furthermore, the event
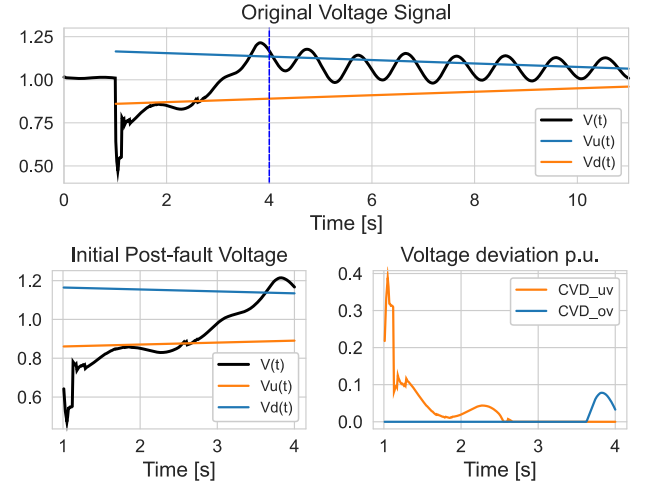

Fig. 7. Example of implementing classification for non-oscillatory events. The upper plot depicts the original voltage signal and upper and lower CVD thresholds introduced in Section III. The lower graphs are the extracted signal interval (left) and the corresponding over- and under-voltage CVD (right).

needs to be sufficiently severe so that it is considered a FIDVR or an STVI event. This is ensured by the second condition shown in (14), i.e., the voltage being at least 1% below the $V_D(t)$ curve for 3 seconds. The proposed thresholds are based on extensive simulations and fundamental characteristics of typical FIDVR and STVI dynamics in various system conditions [3], [27].

The methodology is illustrated in Fig. 7, once again on the combined instability scenario number 15 (see Section IV). The FIDVR event that takes place in the first few seconds after the fault is of interest. The upper plot in Fig. 7 depicts the original voltage signal, as well as the $V_U(t)$ and $V_D(t)$ curves, described in Section III. The blue dashed vertical line represents the cut-off time for the algorithm evaluation. The lower plots show the initial post-fault voltage of interest (left), and its corresponding voltage deviation chart in per-unit values (right). The curves and plots are further explained in Section III.

Once both conditions in (13) and (14) are met, it can be considered that one of the non-oscillatory events (either STVI or FIDVR) is taking place, i.e., a delayed voltage recovery is present; however, it does not reveal which one.

As the main difference between FIDVR and STVI is in the voltage recovery, a simple check of whether the voltage crosses $V_D(t)$ curve throughout the total duration of the evaluation is employed, as shown in (15).

$$V(t) < V_D(t), \quad \forall t \in [t_f + 0.3, \ t_f + 10] \tag{15}$$

If the condition is not true, the voltage has been depressed but it has eventually recovered, indicating FIDVR. If the condition is true, i.e., $V(t)$ is lower than $V_D(t)$ for every t, the prolonged voltage depression is present. This likely results in a partial or total voltage collapse, i.e., STVI. Once again, the first 300 ms of the signal are ignored to reduce the impact of the initial (post-)fault transients on the classification accuracy.

The introduced methodologies for oscillatory and non-oscillatory events jointly form the classification algorithm. The accuracy of the algorithm is tested in the next subsection.
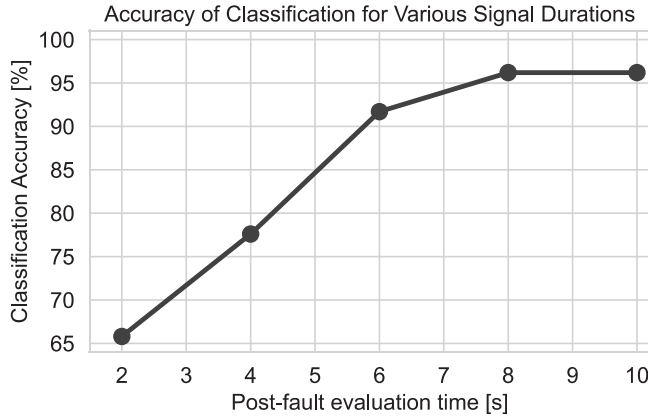
Fig. 8. Classification accuracy for various post-fault evaluation times.

B. Classification Accuracy Results

To test the accuracy of the classification algorithm, the 100 instability scenarios from Section IV are analysed. The classification accuracy is calculated using the well-known expression (16), where TP and TN are the numbers of True Positive and True Negative classifications, and FP and FN are False Positives and False Negatives, respectively [43].

$$Accuracy\,(\%) = \frac{TP + TN}{TP + TN + FP + FN} \quad (16)$$

Furthermore, to evaluate the robustness of the classification methodology for shorter simulation times, tests are conducted not only for a 10-second post-fault duration, but also for 8, 6, 4, and 2 seconds, respectively. These tests are conducted for all 100 scenarios from Section IV, resulting in a total of 500 classification tasks. The benefits of a potentially faster classification are twofold. For offline simulations dealing with system planning and analysis purposes, a shorter dynamic simulation time reduces the computational demand and allows faster analysis. For online applications, the ability to classify events promptly is very important.

For the original signal duration of 10 seconds, the classification algorithm performs very well, achieving 96.2% accuracy over the analysed scenarios. Reducing the available interval to 8 or 6 seconds barely affects the accuracy, which remains higher than 91.5%. However, when even shorter time intervals are used (e.g., <5 seconds), the classification accuracy drops, as shown in Fig. 8. This is expected as some events need several seconds to advance enough to be detectable and classifiable, especially in case of FIDVR and STVI. A promising approach to address this reduced accuracy is to apply time-series extrapolation of the voltage to detect the *likely* future trend of the voltage deviation. Unreported preliminary results show that this may improve accuracy notably for shorter time intervals, and is, therefore, a promising topic for future research. As this article deals with the existing data only, extrapolation techniques and their application are out of scope.

The results demonstrated in this section confirm that the proposed classification algorithm shows a high level of accuracy. Furthermore, the efficacy remains high even for shorter post-fault voltage signals, albeit with an expected reduction in accuracy. The classification algorithm, therefore, complements the quantification algorithm well, allowing for a combined automatic evaluation of severity *and* type of short-term instability, regardless of the nature of the event.

VI. CONCLUSION AND FUTURE RESEARCH

This article explores how the structural changes that power systems experience with the proliferation of power electronics affect stability evaluations. As systems inevitably become weaker with higher IBR penetrations, voltage deviations (especially short-term) play a larger role in understanding, describing, and evaluating instabilities. The presently available short-term stability evaluation methods, however, are facing three main challenges. Firstly, they are rarely applicable to modern power systems with a high penetration of IBRs and dynamic loads. Secondly, they usually focus on a single phenomenon, despite instabilities becoming more intertwined. Lastly, they typically offer a binary instability representation, without the quantification of event severity.

In this article, a novel voltage-based method CVD is proposed to mitigate these challenges. By focusing on voltage deviations, the method becomes more applicable to converter-rich systems and various conventional and emerging instability phenomena, including potentially intertwined instability events. Furthermore, the method is able to quantify how severe a certain grid event is, which offers much more insight than a simple binary stability output. The efficacy and applicability of the method are evaluated on a large number of diverse dynamic simulations and instabilities, demonstrating noteworthy improvements compared to available methods.

Additionally, a new classification algorithm is presented for the detection and classification of various types of short-term instabilities using only voltage curves. The algorithm is tested for a large number of scenarios and its good performance with very high accuracy and robustness is validated accordingly. Furthermore, its potential application for both offline and online cases is investigated for various detection time intervals.

The ability to quantify and classify post-fault voltage deviations enables promising future applications. For offline studies, it is possible to quantify how dangerous certain disturbances are for any grid section, providing information on dynamic system strength and resilience. This can be accomplished by performing a large number of dynamic simulations with advanced IBR and dynamic load models, followed by CVD-based regression analysis. Such a simulation-based approach shall be investigated in the authors' follow-up work, as a part of a probabilistic risk-based resilience analysis. By combining this analysis with an accurate and automatic event classification as introduced in this article, system operators can obtain more detailed insights about the types and severity of voltage dynamics and short-term instabilities that their system may encounter.

Additionally, by being able to detect, quantify and classify instability risks in real-time, suitable preventive and/or corrective measures can be taken in real-time to preserve system resilience and minimize risks of cascading faults and potential partial or total blackouts.

REFERENCES

[1] IEEE, "Impact of inverter-based generation on bulk power system dynamics and short-circuit performance," IEEE, Manhattan, NY, USA, Tech. Rep. PES-TR68, Jul. 2018.

[2] IEEE, "Stability definitions and characterization of dynamic behavior in systems with high penetration of power electronic interfaced technologies," IEEE, Manhattan, NY, USA, Tech. Rep. PES-TR77, Apr. 2020.

[3] A. Boričić, J. L. R. Torres, and M. Popov, "Fundamental study on the influence of dynamic load and distributed energy resources on power system short-term voltage stability," *Int. J. Elect. Power Energy Syst.*, vol. 131, 2021, Art. no. 107141.

[4] A. Arif, Z. Wang, J. Wang, B. Mather, H. Bashualdo, and D. Zhao, "Load modeling—A review," *IEEE Trans. Smart Grid*, vol. 9, no. 6, pp. 5986–5999, Nov. 2018.

[5] J. Matevosyan et al., "A future with inverter-based resources: Finding strength from traditional weakness," *IEEE Power Energy Mag.*, vol. 19, no. 6, pp. 18–28, Nov./Dec. 2021.

[6] B. Badrzadeh et al., "System strength," *CIGRE Sci. Eng. J.*, vol. 20, pp. 5–27, Feb. 2021.

[7] A. Boričić, J. L. R. Torres, and M. Popov, "System strength: Classification, evaluation methods, and emerging challenges in IBR-dominated grids," in *Proc. IEEE PES Innov. Smart Grid Technol.*, 2022, pp. 185–189.

[8] WECC Criterion TPL-001-WECC-CRT-3.2, "Transmission system planning performance," 2019.

[9] ENTSO-E, "Parameters related to voltage issues," ENTSO-E guidance document for national implementation for network codes on grid connection, Nov. 2016.

[10] S. A. Siddiqui, K. Verma, K. R. Niazi, and M. Fozdar, "Real-time monitoring of post-fault scenario for determining generator coherency and transient stability through ANN," *IEEE Trans. Ind. Appl.*, vol. 54, no. 1, pp. 685–692, Jan./Feb. 2018.

[11] A. R. R. Matavalam and V. Ajjarapu, "PMU-based monitoring and mitigation of delayed voltage recovery using admittances," *IEEE Trans. Power Syst.*, vol. 34, no. 6, pp. 4451–4463, Nov. 2019.

[12] M. Golshani et al., "Application of phasor-based functionality to HVDC control in reduced system strength," in *Proc. 17th Int. Conf. AC DC Power Transmiss.*, 2021, pp. 44–49.

[13] M. Zarif Mansour, S. P. Me, S. Hadavi, B. Badrzadeh, A. Karimi, and B. Bahrani, "Nonlinear transient stability analysis of phased-locked loop-based grid-following voltage-source converters using Lyapunov's direct method," *IEEE J. Emerg. Sel. Topics Power Electron.*, vol. 10, no. 3, pp. 2699–2709, Jun. 2022.

[14] R. W. Kenyon et al., "Stability and control of power systems with high penetrations of inverter-based resources: An accessible review of current knowledge and open questions," *Sol. Energy*, vol. 210, pp. 149–168, 2020.

[15] T. V. Cutsem and C. Vournas, *Voltage Stability of Electric Power Systems*. New York, NY, USA: Springer, 1998.

[16] S. Adhikari, J. Schoene, N. Gurung, and A. Mogilevsky, "Fault induced delayed voltage recovery (FIDVR): Modeling and guidelines," in *Proc. IEEE PES Gen. Meet.*, 2019, pp. 1–5.

[17] R. Venkatraman, S. K. Khaitan, and V. Ajjarapu, "Impact of distribution generation penetration on power system dynamics considering ride-through requirements," in *Proc. IEEE PES Gen. Meeting*, 2018, pp. 1–5.

[18] Y. Cheng et al., "Real-World subsynchronous oscillation events in power grids with high penetrations of inverter-based resources," *IEEE Trans. Power Syst.*, vol. 38, no. 1, pp. 316–330, Jan. 2023.

[19] M. Glavic and T. Van Cutsem, "A short survey of methods for voltage instability detection," in *Proc. IEEE PES Gen. Meeting*, 2011, pp. 1–8.

[20] F. R. S. Sevilla et al., "State-of-the-art of data collection, analytics, and future needs of transmission utilities worldwide to account for the continuous growth of sensing data," *Int. J. Elect. Power Energy Syst.*, vol. 137, 2022, Art. no. 107772.

[21] A. Boričić, J. L. R. Torres, and M. Popov, "Comprehensive review of short-term voltage stability evaluation methods in modern power systems," *Energies*, vol. 14, 2021, Art. no. 4076.

[22] F. M. Gonzalez-Longatt and J. L. R. Torres, *Advanced Smart Grid Functionalities Based On PowerFactory*. New York, NY, USA: Springer, 2018.

[23] T. V. Cutsem et al., "Test systems for voltage stability studies," *IEEE Trans. Power Syst.*, vol. 35, no. 5, pp. 4078–4087, Sep. 2020.

[24] A. Boričić, J. L. R. Torres, and M. Popov, "Impact of modelling assumptions on the voltage stability assessment of active distribution grids," in *Proc. IEEE PES Innov. Smart Grid Technol.*, 2020, pp. 1040–1044.

[25] Y. Xu, Z. Y. Dong, K. Meng, W. F. Yao, R. Zhang, and K. P. Wong, "Multi-objective dynamic VAR planning against short-term voltage instability using a decomposition-based evolutionary algorithm," *IEEE Trans. Power Syst.*, vol. 29, no. 6, pp. 2813–2822, Nov. 2014.

[26] CIGRE, "Connection of wind farms to weak AC networks," CIGRE, Paris, France, Tech. Rep. WG B4.62 671, 2016.

[27] A. Boričić, J. L. R. Torres, and M. Popov, "Quantifying the severity of short-term instability voltage deviations," in *Proc. Int. Conf. Smart Energy Syst. Technol.*, 2022, pp. 1–6.

[28] S. Pandey, A. Srivastava, and B. Amidan, "A real time event detection, classification and localization using synchrophasor data," *IEEE Trans. Power Syst.*, vol. 35, no. 6, pp. 4421–4431, Nov. 2020.

[29] R. Igual and C. Medrano, "Research challenges in real-time classification of power quality disturbances applicable to microgrids: A systematic review," *Renewable Sustain. Energy Rev.*, vol. 132, Oct. 2020, Art. no. 110050.

[30] M. Sun, I. Konstantelos, and G. Strbac, "A deep learning-based feature extraction framework for system security assessment," *IEEE Trans. Smart Grids*, vol. 10, no. 5, pp. 5007–5020, Sep. 2019.

[31] M. Popov et al., "Synchrophasor-based applications to enhance electrical system performance in The Netherlands," in *Proc. CIGRE Paris Conf.*, 2022, pp. 1–10.

[32] A. Almunif and L. Fan, "PMU measurements for oscillation monitoring: Connecting prony analysis with observability," in *Proc. IEEE PES Gen. Meeting*, 2019, pp. 1–5.

[33] M. Golshani, D. Wilson, S. Norris, I. Cowan, M. H. Rahman, and B. Marshall, "Application of phasor-based funtionality to HVDC control in reduced system strength," in *Proc. 17th Int. Conf, AC DC Power Transmiss.*, 2021, pp. 44–49.

[34] J. D. Follum, "Detection of forced oscillations in power systems with multichannel methods," Pacific Northwest National Laboratory, Richland, WA, USA, Tech. Rep. PNNL-24681, 2015.

[35] D. P. Wadduwage and U. D. Annakkage, "Improving matrix pencil and Hankel total least squares algorithms for identifying dominant oscillations in power systems," in *Proc. IEEE 10th Int. Conf. Ind. Inf. Syst.*, 2015, pp. 13–18.

[36] S. Halpin, R. Jones, and L. Taylor, "The MVA-Volt index: A screening tool for predicting fault-induced low voltage problems on bulk transmission systems," *IEEE Trans. Power Syst.*, vol. 23, no. 3, pp. 1205–1210, Aug. 2008.

[37] A. Matavalam and A. Venkataramana, "PMU-based monitoring and mitigation of delayed voltage recovery using admittances," *IEEE Trans. Power Syst.*, vol. 34, no. 6, pp. 4451–4463, Nov. 2019.

[38] J. W. Cooley and J. W. Tukey, "An algorithm for the machine calculation of complex Fourier series," *Math. Computation*, vol. 19, 1965, pp. 297–301.

[39] P. Kundur, *Power System Stability & Control*. New York, NY, USA: McGraw-Hill, 1994.

[40] G. Rogers, *Power System Oscillations*. New York, NY, USA: Springer, 2000.

[41] M. J. Gibbard, P. Pourbeik, and D. J. Vowles, *Small-Signal Stability, Control and Dynamic Performance of Power Systems*. Adelaide, Australia: Univ. Adelaide Press, 2015.

[42] A. Boričić, J. L. R. Torres, and M. Popov, "Beyond SCR in weak grids: Analytical evaluation of voltage stability and excess system strength," in *Proc. Int. Conf. Future Energy Solutions*, 2023, pp. 1–6.

[43] M. Grandini, E. Bagli, and G. Visani, "Metrics for multi-class classification: An overview," *arXiv:2008.05756*.

Aleksandar Boričić (Member, IEEE) received the Dipl.Ing. degree in electrical power engineering from the University of Montenegro, Podgorica, Montenegro, and the double master's degree from the KTH Royal Institute of Technology, Stockholm, Sweden, and Eindhoven University of Technology, Eindhoven, The Netherlands, in 2019, in the Smart Electrical Networks and Systems Programme. He is currently working toward the Ph.D. degree with the Intelligent Electrical Power Grids Group, Delft University of Technology, Delft, The Netherlands. He completed his M.Sc. thesis research externally with ABB Corporate Research Centre, Västerås, Sweden, in the field of renewables' impact on power system protection. He worked as a Power System Engineer for the TSO of Montenegro and as an electrical engineer/consultant for DNV. His research interests include power system dynamics, stability, system strength, protection, and WAMPAC. He is an active participant of the CIGRE C4/C2.58/IEEE joint working group Evaluation of Voltage Stability Assessment Methodologies in Transmission Systems, and an active CIGRE Member and CIGRE NGN ambassador. In 2023, he joined TenneT TSO B.V. as a Future Grids Operation Developer.

Marjan Popov (Fellow, IEEE) received the Ph.D. degree in electrical power engineering from the Delft University of Technology, Delft, The Netherlands, in 2002. In 1997, he was an Academic Visitor, at the University of Liverpool, Liverpool, U.K., where he conducted research in the field of SF6 arcs, where he is also a Chevening Alumnus. His main research interests include future power systems, large-scale power system transients, intelligent protection for future power systems, and wide-area monitoring and protection. Dr. Popov is a Member of CIGRE and actively participated in WG C4.502 and WG A2/C4.39. He is active in A3 and B5 committees dealing with circuit breakers and protection. He was the recipient of the Hidde Nijland Prize for extraordinary research and education achievements in the field of smart grids in 2010, IEEE PES Prize Paper Award, and IEEE Switchgear Committee Award for 2011 and an Associate Elsevier's International Journal of Electric Power and Energy Systems. In 2017, he founded the Power System Protection Centre in The Netherlands, with the aim to promote research and education in Power System Protection.

Jose Luis Rueda Torres (Senior Member, IEEE) was born in 1980. He received the Electrical Engineer Diploma (*cum laude Hons.*) from Escuela Politécnica Nacional, Quito, Ecuador, in 2004, and the Ph.D. degree in electrical engineering from the National University of San Juan, obtaining the highest mark 'Sobresaliente' (Outstanding) in 2009. He is currently an Associate Professor leading the research team on Resilient Sustainable Energy Systems, within the Intelligent Electrical Power Grids Section, Electrical Sustainable Energy Department, Delft University of Technology, Delft, The Netherlands. From 2003 to 2005, he was at Ecuador, in the fields of industrial control systems and electrical distribution networks operation and planning. Between 2010 and 2014, he was a Postdoctoral Research Associate at EAN. His research interests include stability and control of power systems and multi-energy systems, power system operational planning and reliability, and probabilistic and artificial intelligence methods. He is currently a Member of the Technical Committee on Power and Energy Systems of IFAC (International Federation of Automatic Control), Chairman of IEEE PES Working Group on Modern Heuristic Optimization, Secretary of CIGRE JWG C4/C2.58/IEEE Evaluation of Voltage Stability Assessment Methodologies in Transmission Systems, Secretary of the IEEE PES Intelligent Systems Subcommittee, and Vice-Chair of the IFAC Technical Committee TC 6.3. Power and Energy Systems on Social Media.